Preferred citation: D.W. Coffin, K. Li and J. Li. Utilization of modified linear elastic fracture mechanics to characterize the fracture resistance of paper. In **Advances in Pulp and Paper Research, Cambridge 2013**, *Trans. of the XVth Fund. Res. Symp. Cambridge, 2013*, (S.J. I'Anson, ed.), pp 637–672, FRC, Manchester, 2018. DOI: 10.15376/frc.2013.2.637.

UTILIZATION OF MODIFIED LINEAR ELASTIC FRACTURE MECHANICS TO CHARACTERIZE THE FRACTURE RESISTANCE OF PAPER

Douglas W. Coffin[1], Kun Li[2] and Ji Li[1]

[1] Department of Chemical and Paper Engineering, Miami University, Oxford OH 45056 USA

[2] Metso USA, Norcross, GA 30071 USA

ABSTRACT

Linear elastic fracture mechanics modified to account for an effective fracture process zone is sufficient to characterize and predict fracture resistance for a wide range of papers. The simplicity of the method, which only requires the tensile strength and a measure of the effective fracture process zone length, gives it great advantage over other existing approaches. The results presented here show that for a wide range of commercial papers, samples widths as narrow as 50 mm are sufficient to determine the effective process zone length, and that scaling holds well enough to allow prediction for fracture of wide webs. The results indicate that the tensile strength of paper is a result of a fracture process where the defect is most typically induced from cutting the network structure along the edges. As a consequence, the inherent tensile strength of the network can be significantly larger than the measured tensile strength. The effective fracture process zone length parameter is taken as a measure of the inability for the paper to concentrate load near the crack tip. This ability for network structures to concentrate load has significant impact on the fracture resistance of the sheet relative to its tensile strength.

1 INTRODUCTION

Imperfection limits the strength of paper, but this defect sensitivity is tempered by dissipative material and structural processes and features that limit the ability of the sheet to concentrate load. A substantial amount of literature has been devoted to understanding the fracture resistance of paper; see the reviews of Kortschot [1], Mäkelä [2], and Niskanen [3]. A recent account of the requirements, advantages, disadvantages, and applicability of Linear Elastic Fracture Mechanics [LEFM], nonlinear fracture mechanics, cohesive zone modeling and damage mechanics was provided by Östlund and Mäkelä [4]. It is clear that, LEFM in a strict sense cannot be applied to paper. Uesaka et al. [5] first showed that the J-integral method was better suited for characterization of fracture in paper compared to the stress-intensity factor. At the 10th FRS, Niskanen [3] concluded that LEFM cannot generally be applied to paper. He concludes that LEFM is reasonable only for cases where the crack sizes are sufficiently large to render the plastic fracture process zone negligible and this requirement results in unreasonably large test specimen sizes. Östlund et al. [6] point out that LEFM even with a plastic zone correction is not self-consistent, because a measure of rupture energy over predicts the stress intensity factor and a measure of stress intensity under predicts rupture energy. Despite this fact, there is still evidence in the literature [7–9] that LEFM methods are useful for characterization of fracture resistance.

Andersson and Falk [10] used a Griffith-Irwin type fracture criteria to account for the undefined fracture process zone (*FPZ*) that precedes the well-defined crack [11]. They did not correct for the finite-width of their samples (15 mm), which is likely too small to fully capture the behavior [12] and it would seem that they under-predict the *FPZ* (0.6 mm for handsheets). They also conducted constant load fracture tests on larger width samples, and the resulting *FPZ* seems to be approximately four times larger (on the order of 2.5 mm for handsheets.) Seth and Page [7] utilized LEFM to study the fracture behavior of paper and conclude that for LEFM to be applied to paper, the samples must be of sufficient sample width and crack length. Swinehart and Broek [8] showed that LEFM equations can predict fracture loads of large webs with large cracks with no modification for the *FPZ*.

Donner [9] continued in the same vein as previous work [7, 10] and separated the *FPZ* into a structural and material component. By conducting tensile tests on newsprint samples in a cryogenic environment, a very brittle and linear-elastic response was obtained. Fracture tests in the cryogenic environment yielded a *FPZ* of about 0.5 mm for MD and 1.1 mm for CD. At room temperature, the *FPZ* was 1.5 mm for MD and 3.7 mm for CD.

Kortshot and Trakas [13] took a similar approach, point stress criteria (PSC), to describe the fracture resistance, utilizing both centered holes of various diameters and centered slits for newsprint, bond paper, and a copy paper. For holes they found the characteristic *FPZ* length to be in the range of 1.2 to 1.7 mm for MD and 3.3 to 3.5 mm for CD. For slits, the characteristic length in MD was smaller, 0.8 to 1.0 mm, which could have been affected by the expression they chose to use for the stress-distribution near the slit. Inspection of their results shows that the strength of a sheet with a 1 mm hole was not significantly different than the tensile strength indicating that the small hole did not affect the ability to the paper to effectively carry load; indicative of Donner's [9] structural *FPZ*. Considine et al. [14] utilized the PSC and an average stress criteria (ASC) along with LEFM equations for the stresses near a hole for an orthotropic material. These authors do not report the *FPZ*, but do report inherent flaw sizes ranging from 0 to 0.88 mm for MD and 0 to 1.55 mm for CD for a range of papers.

The attractiveness of LEFM is the simplicity of its application; an argument proffered by Swinehart and Broek [8] for favoring stress intensity factor over the J-integral method. An abundance of explicit equations are available for LEFM, and if applicable one could apply these equations to characterize paper materials and predict behavior with increased size-scaling with relative ease. Implementing nonlinear fracture mechanics is complex; requiring a description of the constitutive behavior, a library of stored geometric correction factors, and numerical evaluation for each point of interest. To be useful the LEFM method should be capable of predicting the behavior of large samples from measurements made on small samples.

Using nonlinear fracture mechanics, Mäkelä, Nordhagen, and Gregersen [15] demonstrated that they could predict the behavior of wide samples (800–1000 mm) based on fracture toughness measurements of narrow samples (50 mm). Expanding on the approach of Swinehart and Broek [8] for a J-integral method, Mäkelä and Fellers [16] and Mäkelä [17] have presented procedures and explicit equations that can be used for prediction of fracture resistance. While it eliminates the need to complete a finite-element analysis, it still requires a library of correction values, and numerical inversion for each prediction.

Östlund and Mäkelä [4] state the following: "Many fracture mechanics models can be applied to paper materials and products depending on the problem and objectives of the analysis, but is it best to use the simplest possible model that has predictive capability." The simplicity of LEFM is too attractive to completely dismiss and despite its reported shortcomings it may still be valuable as a predictive tool that can be implemented with minimal testing and little computational difficulty. Although LEFM is stated to be adequate for large sheets with large cracks, it remains to explore its applicability for smaller cracks and predictions based on independent measures. Reporting the results of such an inquiry is one of the main purposes of this contribution.

In the following, the LEFM equations are modified with the addition of an inherent *FPZ* and a normalization to the tensile strength. The previous literature is considered in light of this approach, and the predictive capability using the data from [15] is shown to be just as adequate as the nonlinear fracture mechanics approaches used in [15–17]. By assuming that tensile strength is governed by the same fracture process, the singularity for small cracks sizes is removed, or rather a finite length crack is always present. The interpretation of the *FPZ* presented here is as a measure of the inability of the paper to concentrate load at the crack-tip. The larger the *FPZ* the less ability the structure and/or material has to concentrate load at the tip and the higher the fracture toughness relative to the tensile strength. Results are provided to demonstrate how the relative defect sensitivity of papers can be assessed. This development provides a simple method that can be utilized to characterize the fracture toughness of materials and predict the behavior in large webs; at least with small cracks.

2 ANALYSIS

2.1 Modified LEFM

Because paper is a discrete network structure of fibers, it is inherently flawed. There is a scale level below which the assumptions of continuity are invalid. The discrete nature of paper is smoothed because it is stochastic and continuum models can be applied to great success as long at the dimensions of interest are relatively large. With regards to fracture, previous fracture studies [9, 13, and 14] indicate that this inherent flaw is on the order of a few millimeters. The governing equations for an ideal elastic continuum, allow for singular stresses, but in real materials they are limited to some finite maximum. For a brittle response, the stress is limited by this minimum structural scale, and if the failure mechanism is a fracture process, we can cut-off the singularity by normalizing the fracture loads to the strength based on a minimum allowable crack size.

Most papers exhibit sensitivity to cracks or notches, but tend to be relatively tough materials. Notch sensitivity is typically attributed to a concentration of stresses near the tip of the notch. There is a zone around the notch where the material has yielded and/or undergone partial failure. At some level of loading, the material fails globally; typically starting near the notch tip. The maximum load could correspond to the point when the notch length begins to increase or shortly after that event. Inside the zone of influence near the crack tip, a multitude of mechanisms could be occurring to diminish the stress concentrations. Plasticity will limit magnification of stresses. Cohesive failure of the structure will allow reduction of stress levels. The inherent structural inhomogeneity will create some scale level below which stresses cannot concentrate. The literature includes successful application of theories that account for one of these aspects while ignoring others; for example see [15] for plasticity and [18] for material heterogeneity. In these models, some parameter is utilized to account for the effective behavior of the material regardless of the actual contribution from various different effects.

In-plane, fracture tests geometries are typically conducted as either a center-notched test (CNT), a double edge-notched test (DENT), or a single edge-notched test (SENT) with specimens as shown in Figure 1. The geometries are defined for each test such that the ligament length to sample width ratio is $1-a/w$ and that for small cracks the SENT and the DENT would converge to the same fracture strength for the same magnitude of a. Note, this requires that for SENT the width, W, is defined as $W=w$ instead of $2w$. For the cases considered here the notch or crack, a, is considered a slit, with the tip as sharp as the minimum discrete size scale permissible in the structure. The sample is loaded in tension with a load F. Force equilibrium requires that the net force on the remaining ligament must still equal F, but if stresses are higher at the notch tips the failure load reached in fracture will be reduced more so than the reduction in ligament length.

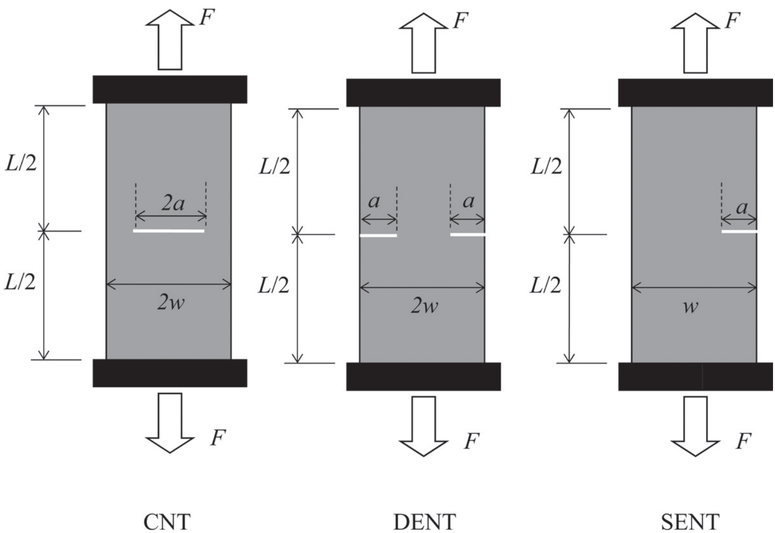

Figure 1. Typical geometries for in-plane fracture tests with paper.

Notch sensitivity can be assessed by comparing the ratio of ultimate load of the specimen, F, to that of the un-notched specimen, F_0. The criterion is

$$\frac{F}{F_0} < 1 - \frac{a}{w} \text{ implies specimen is notch sensitive.} \tag{1}$$

An equality sign in Equation (1) would imply no sensitivity to the notch, and a greater than inequality would imply the notched specimen is effectively stronger than a specimen whose width equals the ligament length. For a material, whose strength is determined by defects one would expect the load ratio to exceed one as the ligament length approaches 2**FPZ* because if stresses are elevated at a crack tip, the inherent strength must be greater than the bulk tensile strength.

Consider a linear elastic material. Following classic LEFM, the stress intensity factor can be expressed as [19]

$$K_I = \sigma\sqrt{\pi a}\, f(a/w) \tag{2}$$

where σ is the far field stress and $f(a/w)$ is a correction factor for finite width samples. In Equation (2), the length is assumed to be sufficiently long as to not influence the correction factor. Expressions for the correction factors for the three geometries given in Figure 1, reported to be valid for all $x<1$ [19] are:

$$\begin{aligned}
&\text{for CNT:} \quad f(x) = \left(1 - 0.025x^2 + 0.06x^4\right)\sqrt{\sec(\pi x/2)} \\
&\text{for DENT:} \quad f(x) = \left[1 + .122\cos^4(\pi x/2)\right]\sqrt{\frac{2\tan(\pi x/2)}{\pi x}} \\
&\text{for SENT:} \quad f(x) = \frac{\left[0.752 + 2.02x + 0.37\left(1 - \sin(\pi x/2)\right)^3\right]}{\cos(\pi x/2)}\sqrt{\frac{2\tan(\pi x/2)}{\pi x}}
\end{aligned} \tag{3}$$

Note the ratio of center to edge notched correction factor for x going to zero is 1.122 (The precision reported here is the same as given in [19], experimental significance is accounted for in the determination of d). If we assume that failure occurs when the stresses at the tip reach some failure level, it implies that the stress intensity factor, K_I, is constant for all crack sizes and Equation (2) can be inverted for a>0. Now we assume that paper has an inherent characteristic fracture process zone length, d, such that the un-notched limit load can be obtained from Equation (2) as

$$F_0 = \frac{K_I W t}{f(d/w)\sqrt{\pi d}} \tag{4}$$

where t is the thickness. Then the limit load ratio for at any notch $a>d$ can be written as

$$\frac{F}{F_0} = \frac{f(d/w)}{f((a+d)/w)}\sqrt{\frac{d}{(a+d)}} \;\; \forall\ a < w - 2d. \tag{5}$$

The length d is assumed to be composed of both a structural component and a material component $d = d_s + d_m$. Consider the structural component a result of the discrete nature of the fiber network structure. The length d_s could be treated as in inherent "flaw". In the presence of these flaws, edge failure would be more likely in a tensile test because load transfer structure is open at the edges. In addition, comparison of Equation (3) for CNT, DENT, and SENT shows that for small notches edge-notched specimens fail at a lower load then center-notched samples. In addition, both edges would have these flaws so the tensile strength should be similar to the DENT geometry except with small flaws.

For cracks $a<d_s$, the fracture load should remain equal to F_0. Thus, equation (5) can be modified to be written as

$$\frac{F}{F_0} = \begin{cases} 1 & \forall a \le d_s \\ \dfrac{f(d/w)}{f(a+d-d_s)/w)}\sqrt{\dfrac{d}{(a+d-d_s)}} & \forall d_s < a < w-2d \end{cases} \tag{6}$$

The load ratio is equivalent to the average far field stress ratio and thus equation (6) provides a prediction for the fracture resistance of a paper. For edge cracked samples, the far-field fracture stress, σ_f can be predicted from the tensile strength, *TS*, the characteristic fracture process zone length, d and the structural limit, d_s. as

$$\sigma_f = TS \begin{cases} 1 & \forall a \le d_s \\ \dfrac{f(d/w)}{f(a+d-d_s)/w)}\sqrt{\dfrac{d}{(a+d-d_s)}} & \forall d_s < a < w-2d \end{cases} \tag{7}$$

If center-notched specimens are used, the limiting ratio of failure stress to tensile strength at zero-notch length would be 1.122 because the un-notched specimen is more likely to fail at an edge rather than the center.

Figure 2 illustrates the effect of d on the load ratio using equation (6). Figure 2a is for the case where the characteristic fracture zone length is $d=d_s$, and Figure 2b illustrates the case where $d_s=0$. Any combination between the two sets of curves can be obtained by adjusting the proportion of d_s to d.

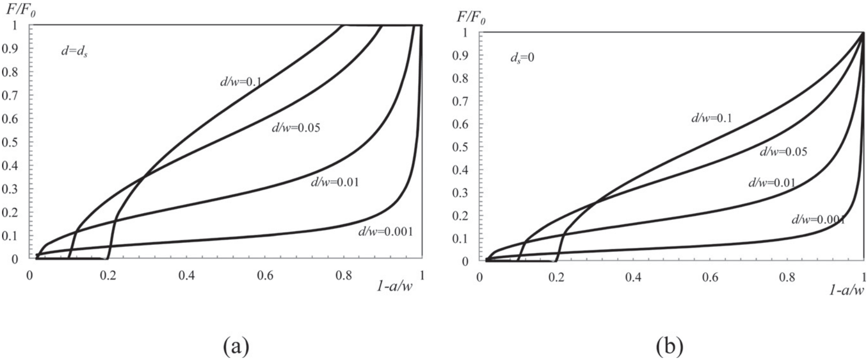

Figure 2. Fracture load ratio as a function of ligament length for various characteristic fracture lengths for DENT. (a) All structural $d=d_s$, (b) all material $d_s=0$.

By re-casting the LEFM equation as shown in Equation (7), two important features missing from classic LEFM are gained. First, instead of relying on a measure of released and consumed energy as a measure of fracture toughness, Equation (7) relies on the tensile strength of the sample for magnification and a determination of *FPZ=d* for the relative sensitivity of the material to defects. Second, the stress singularity at the crack tip is removed or rather irrelevant. The assumption of a nonzero *d* and constant stress intensity factor ensures that the predicted load will converge to the tensile strength as the crack length goes to zero.

Equation (6) or (7) is a modified LEFM model that can be used to characterize and predict the fracture sensitivity of paper. The *FPZ* parameter *d* provides a measure of fracture sensitivity relative to the strength of the material. For specimen widths sufficiently larger than $2d$, $f(d/w)$ is approximately $f(0)$ and the stress intensity factor can be defined as

$$K_I = 1.122 TS\sqrt{\pi d} \tag{8}$$

The corresponding elastic energy release rate for an isotropic material is

$$R = \frac{K_I^{\,2}}{E} = 1.259\pi \frac{TS^2 d}{E} \tag{9}$$

For an orthotropic material, the effective modulus can be taken as $E = E_{11}^{\,3/4}\, E_{22}^{\,1/4}$, where E_{11} is the elastic modulus in the load direction and E_{22} is the elastic modulus in the direction perpendicular to the loading [6].

2.2 Fracture of a Flawed Elastic Lattice

To demonstrate the effect of a discrete structure on the fracture sensitivity, a lattice model was developed using MATLAB. The model is shown to the left in Figure 3. The elements were assumed to be linear springs, but large deformations were accounted for with a quasi-static time step updating the length and orientation of the elements with each incremental loading. The lattice is composed of nodes arranged in a square array with the characteristic length *c*. The springs are arranged to be horizontal, vertical, and diagonal. The diagonal elements are not connected where they cross. The stiffnesses are chosen to give an initial isotropic response. Along the top edge the nodes are displaced with a uniform vertical displacement and free to move in the horizontal direction.

Along the bottom horizontal axis of symmetry, the last node is not connected to the line of symmetry. This is the initial flaw and renders the model a DENT. Additional crack lengths of length *a* are given by releasing the nodes to the right of *a* from being held to the line of symmetry. The vertical displacement along the top is incrementally increased until the reaction force at the crack tip (node furthest to the right being held to the horizontal line of symmetry) reaches a specified value. The model can easily be adjusted to be orthotropic, allow for plasticity of the elements, or a cohesive release of the nodes fixed to the horizontal line of symmetry. The deformed lattice shown to the right in Figure 3 corresponds to 120 steps to reach 10% effective strain, with a/w=0.4.

The initial state is taken with just the right corner node released. The applied force is obtained by summing the reaction forces, which are vertical, along the top edge. Then the model is re-run, but the next node to the left is released, effectively doubling the crack size. The load ratio is then determined for each crack size. If one imagines the crack size to be continuous, then the results of load ratio versus crack length will give a stair-step function. The load remains constant for all crack lengths between two nodes, and has a step discontinuity at a crack length corresponding to a nodal location.

Figure 4 provides the results of two simulations, which illustrate the behavior of the model. Figure 4a corresponds to a lattice with 5 unit cells in the half-width and 25 unit cells in the half-length so that the characteristic length ratio is c/w=0.2. Figure 4(b) corresponds to a model with a characteristic length ratio of c/w=0.1 by using 10 unit cells in the width direction and 50 in the half-length direction. In Figure 4a, the stair step response of the lattice model is shown. The circle markers represent the model result. The square markers represent the average of the two values at a node. The curves are representative of Equation (6) with three proportions of d_s to d. The upper solid curve represents d_s=0, the bottom dashed curve represents d_s=c, and the middle dash-dot curve represents d_s=c/2. For all three lines, the characteristic *FPZ* is d=c.

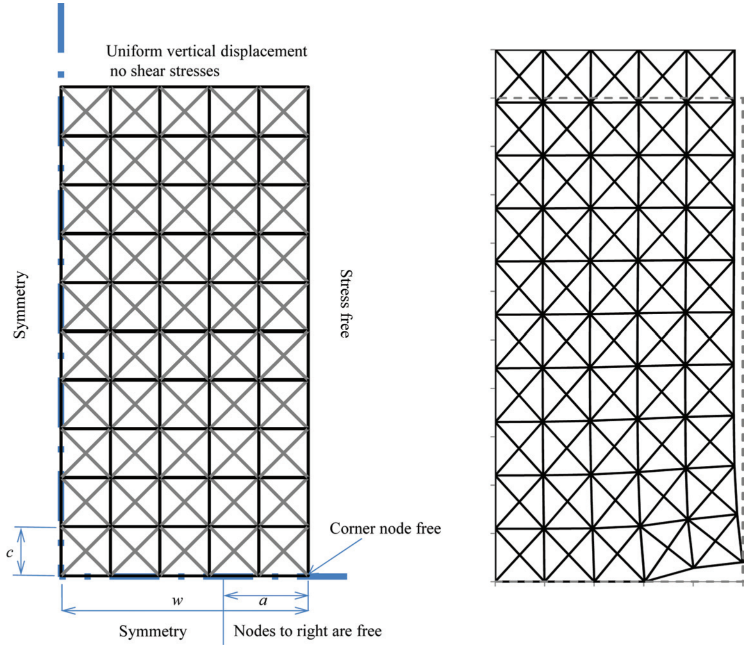

Figure 3. Flawed lattice model (1/4 of DENT specimen). (Right: deformed lattice)

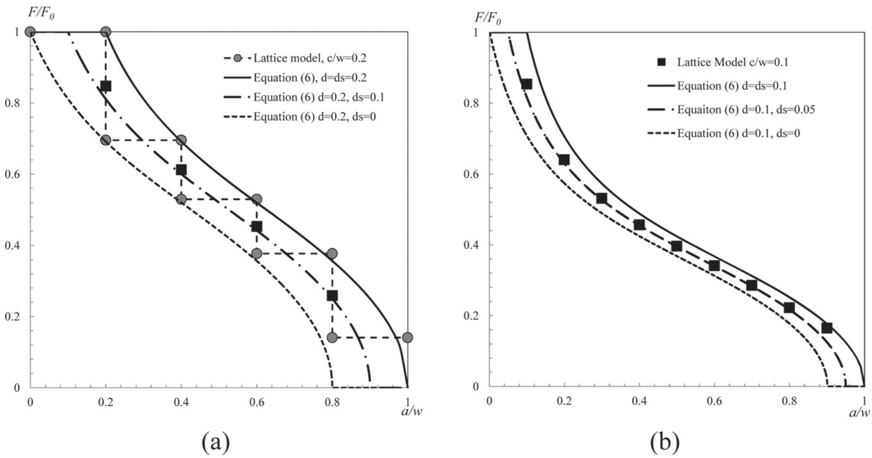

Figure 4. Load ratio versus crack length for flawed lattice model. Black squares represent the average load ratio that occurs before and after the release of a node at a crack length of *a*. (a) is for a lattice with *w*=5*c* and *L*=50*c*, and (b) is for *w*=10*c* and *L*=100*c*.

Figure 4b shows only the average points from the lattice model, but the three corresponding curves from Equation (6) for d_s=*c*, d_s=*c*/2, d_s=*c* are given. As the ratio *c*/*w* decreases, the three curves will converge and the sensitivity to cracking will increase. Equation (6) with d=2d_s=*c* provides an excellent fit of the numerical results. A comparison of the two curves is given in Figure 5.

The length of *c* relative to the width determines the ability of the structure to concentrate load. Figure 6 compares the stress distribution for the case when the crack length is *a*/*w*=0.4 for the lattice models having *c*/*w*= 0.05, 0.1, and 0.2. With the smaller lattice structure, the stresses can concentrate closer to the tip. This is why the smaller lattice exhibits more sensitivity to cracks.

Thus, for an elastic material the parameter *d* represents a measure of the inability of the structure to concentrate load. Plasticity would further limit stress concentrations and increase the effective *FPZ, d*.

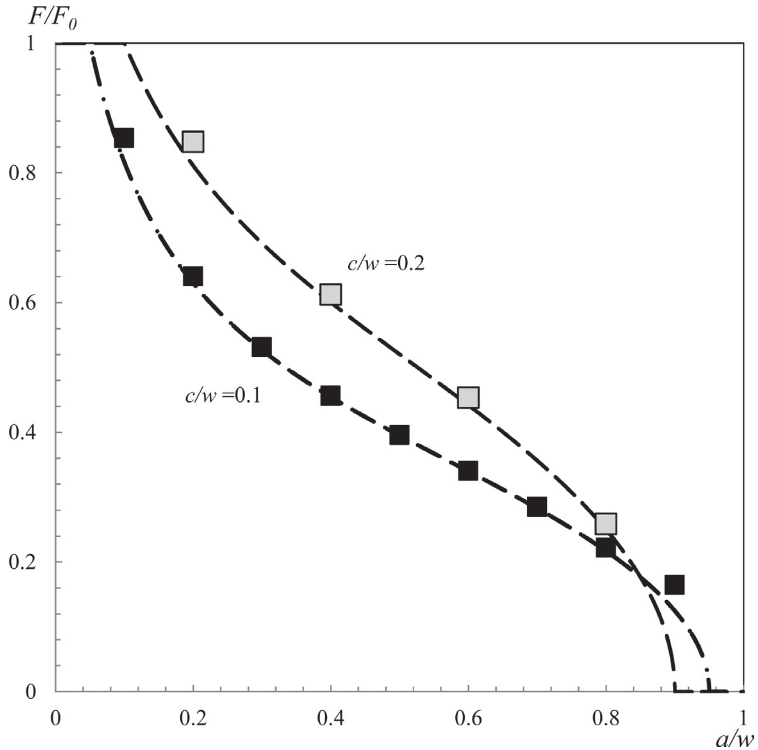

Figure 5. Effect of characteristic lattice structure size on sensitivity to fracture.

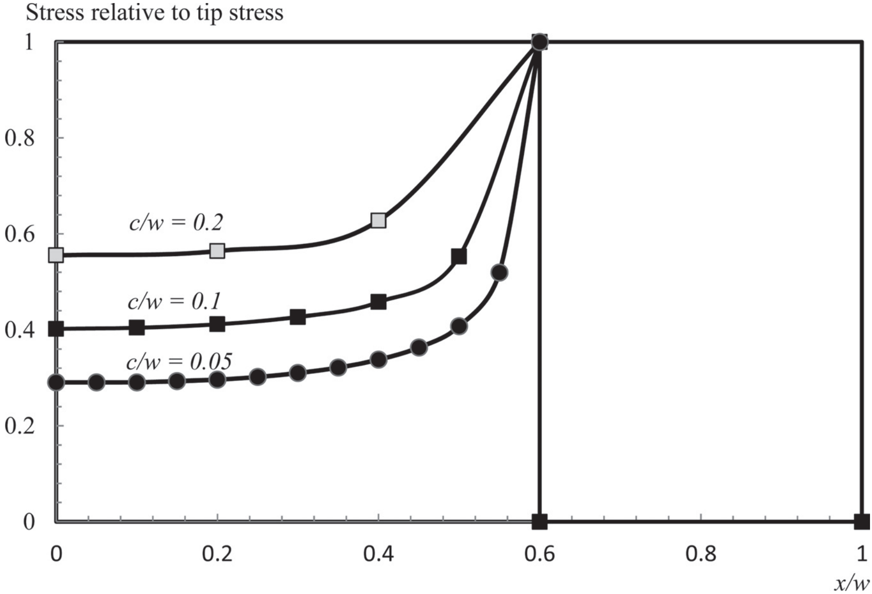

Figure 6. Stress distribution along ligament for three characteristic lattice sizes with a/w=0.4.

3 RELEVANCE TO THE LITERATURE

It remains to be seen if Equations (6) or equivalently (7) are useful to characterize the fracture sensitivity of a paper and is capable of predicting the fracture of large webs based on values obtained from small scale testing. It is worth re-examining the data in the literature to evaluate Equation (6) or (7). For most of these comparisons, the term d_s is set to zero because not enough information is available to distinguish it from d. This means that the data from the literature is typically fit with two parameters, tensile strength (*TS*), and the effective *FPZ* (*d*).

Östlund et al. [6] determine that LEFM could not be used to predict fracture. To make their argument, they used DENT specimens of a copy paper with 2, 4, and 6 mm notches and a sample width of either 100 or 50 mm. They report both the critical fracture stresses and the tensile strength of the samples. This fracture load to tensile strength ratio data is shown in Figure 7 along with a fit of Equation (7) where the parameter d is the fitting parameter. For MD was found to be d=2mm and for CD d=5 mm. Östlund et al. [6] calculated stress intensity factors from two methods. Directly from the fracture strength and from the fracture energy determined from a short span tensile test. They then determined values of

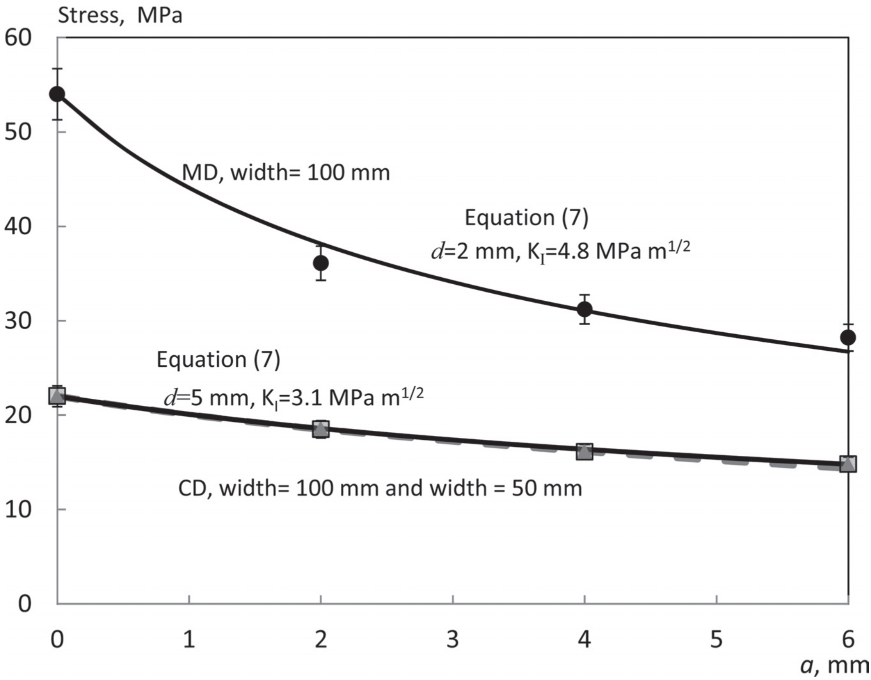

Figure 7. DENT fracture tests of a copy paper [6] compared to Equation (7).

d to minimize the error in the fracture stress calculation. A comparison of the current fit to that found in [6] is given in Table 1.

Figure 7 illustrates that Equation (7) provides reasonable fit for the fracture strength. The fact that the same *d* fits for both the 50 and 100 mm lengths in CD suggests Equation (7) can be used when scaling to larger samples. In other words, for these crack lengths the shape factor is approximately constant as

Table 1. Comparison of parameters from Equation (7) and reference [6]

	d, mm		*K_I MPa $m^{1/2}$*			*R, kJ/m²*	
	Eq. (7)	*Ref. [6]*	*Eq (8)*	*Ref. [6] stress*	*Ref. [6] energy*	*Eq (9)*	*Ref. [6]*
MD	2	8.0	4.8	3.2–4.4	7.4	4.3	10.2
CD	5	11.7	3.1	1.6–2.3	4.7	2.8	6.5

sample width increases beyond 50 mm. The fact that the tensile strength (zero notch) fits with the other fracture data suggests that one does not need a separate measure of fracture energy. The stress intensity factors determined from the short-span tensile test are large. The values of K_I= 4.8 and 3.1 MPa $m^{1/2}$ from the current analysis are very similar to the results given by Swinehart and Broek [7] for papers with similar tensile strength in MD and CD. Clearly, using the fracture energy calculated from a short-span tensile test causes an over prediction of fracture resistance from LEFM methods for short cracks. The equivalent elastic fracture energy determined from Equation (9) is about 40% of that reported in [4]. There is no reason to expect the LEFM methods, which utilize an effective *FPZ*, to match the actual energy release, which consumes energy to drive the plastic front. One would expect it to be less than such a measured value. Also, the short span measurement would be valid for deep notches and this could require higher energy than that required to propagate a small crack. This fit shown in Figure 7 does not require an input of fracture energy to be predictive. It requires the tensile strength and at least one fracture test to determine the value of *d*. The results shown in Figure (7) support the assumption that the tensile strength of an un-notched sample is also a result of fracture and that this measure gives us the necessary magnification factors to scale the load ratio factor. Thus, Equations (7), (8) and (9) have validity. Donner [9] also found that the tensile strength was aligned with the fracture data.

Seth and Page [7] attributed the low energy calculated in the work of Anderson and Falk [10] to the small sample width. The one example of fracture load versus notch depth given by Anderson and Falk [10] was in their Figure 4, which is re-plotted in Figure (8). Anderson and Falk [10] plotted the stress squared as a function of $1/a$, which should give a line. Anderson and Falk did not correct for the finite width of their samples. The circle markers in Figure 8 represent corrected values based on Equation (6). Figure 9 shows the stress versus notch length as well as the average ligament stress versus notch data. The stress is normalized to the fracture stress for the smallest notch. Figure 9 reveals that the average ligament stress for the two largest notches exceeds the average stress of the smallest notch. Because of the narrow samples used by Anderson and Falk [10] one might expect that the two deepest notches give results that are not indicative of the fracture resistance, but rather significant yielding across the entire ligament length would allow a higher load to be reached before failure. Anderson and Falk [10] reported a d=2.5 mm for handsheets tested with larger width. If this value is used in Equation (6), the two deepest notches are excluded, and the slope is adjusted to pass though (0, 0), the square of the stress intensity factor doubles (see Figure 8). This would then give a fracture energy at about 40% of that reported by Seth and Page [7]. This is similar to the percentage differences reported by Östlund et al. [6].

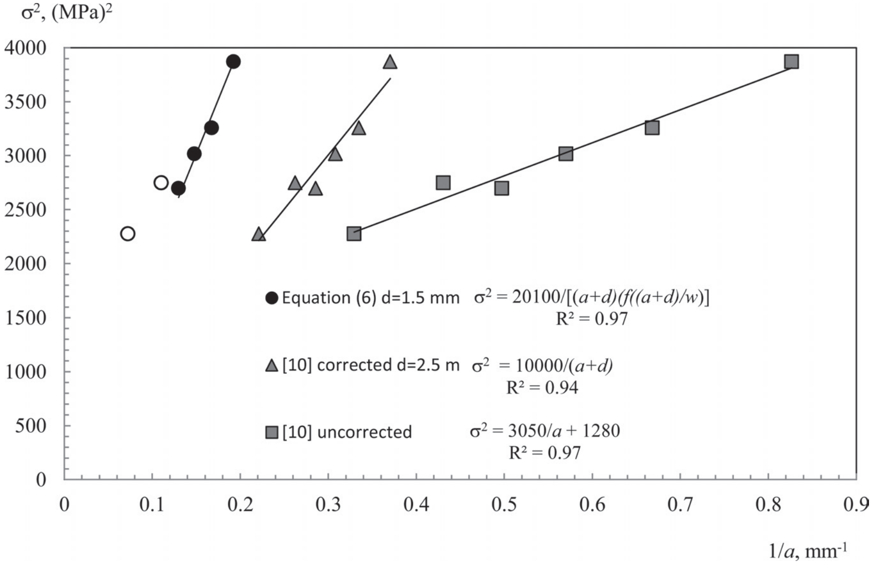

Figure 8. Fracture results from Fig 4 of Ref. [10] and Equation (6) with d=2.5 mm.

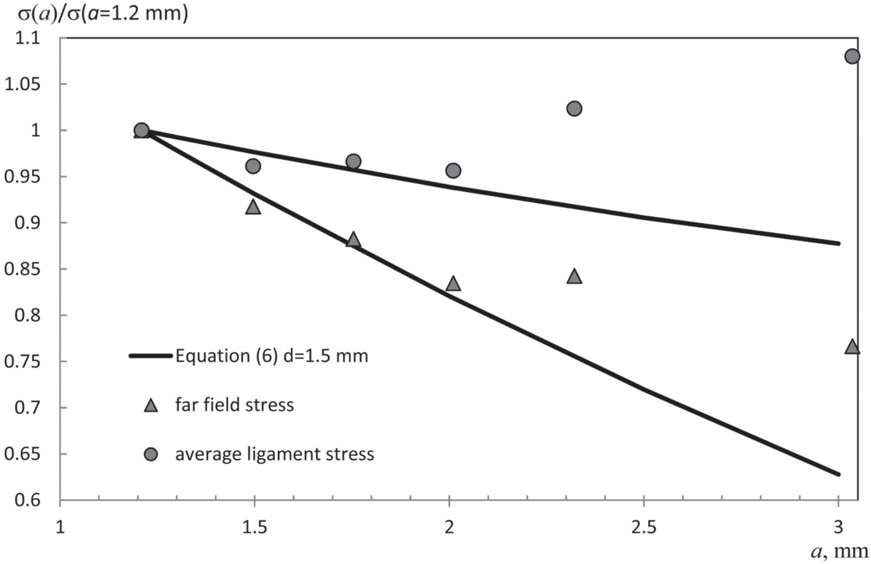

Figure 9. Relative far field stress level and average ligament stress for data from [10].

Seth and Page [7] reported a match in energy release rates from fracture tests and short-span notched tensile tests for large width DENT, having an aspect ratio a/w=0.4. In the short webs, they had a length to width ratio of three, but the ratio was one for the larger webs. Given that they tested in MD, the aspect ratio of unity could give a sufficiently different response than the aspect ratio of three. It does not appear that they used a correction factor for length to width to account for the fact that a uniform far-field stress may not be obtained with the length to width ratio of one. Thus, the agreement that Seth and Page observed may not hold for sufficiently long sample lengths.

Swinehart and Broek [20] present failure load versus crack length data from CNT for two papers in their Figure 4. This figure is recreated in Figure 10, where the load has been scaled to the tensile strength and the crack to half-width ratio is used. The dashed lines represent the LEFM fit from [20] and the solid lines represent the prediction from Equation (7). The values of d given in Figure 10 were calculated from Equation (8) using the stress concentration factors and the tensile strengths reported in [20]. Equation (7) fits they data as well or better at all points compared the LEFM fit. The largest improvement is for small cracks, where Equation (7) converges to a value of 1.122*TS*. This comparison shows that the modified LEFM can improve the ability to describe the fracture data at small crack lengths.

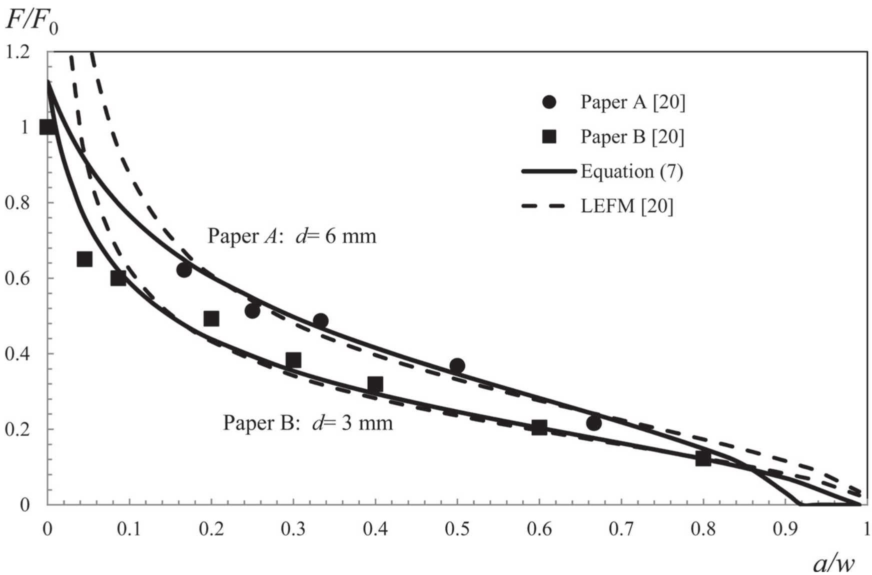

Figure 10. Comparison of Equation (6) to LEFM using CNT data from [20].

The data of Mäkelä, Nordhagen, and Gregersen [15] can be used to determine if Equation (7) has predictive capabilities. Tensile and fracture test results for these papers were reported in [15, 16, and 17]. The fracture test was on a 50 mm wide sample with a center notched crack, with a/w=0.4. Table 2 provides this data along with the value of d determined from Equation (7) and the fracture toughness index JI_{cr} reported in [17].

The measure of d given in Table 2 was determined by setting F/F_0=1.122F/ $(gr \cdot TI \cdot W)$ and using the solver in Excel to determine the value of d, which satisfied the equality. Mäkelä et al. [15] completed SENT fracture tests on large webs with widths of W= 800–1000 mm for the papers listed in Table 2. Figure 11 provides the predictions from Equation (6) compared to the data [15]. An additional prediction using the approach outlined in Mäkelä [17] provides four points, a/W= 0.005, 0.01, 0.015, and 0.025, of a curve based on nonlinear fracture mechanics analysis. To determine these points, the tabled-factors given in [16, 17] along with the material properties shown in the corresponding graph of Figure (11), were used to determine the load ratio. For each point, the Excel solver was utilized to determine the load factor. Inspection of the graphs shows that the prediction of the modified LEFM equation is as good as the prediction from nonlinear fracture mechanics. Inspection of the predictions from nonlinear fracture mechanic combined with finite element analysis obtained in the original work [15] shows that the prediction from LEFM prediction is just as adequate.

Mäkelä [17] provided predictions for CD fracture tests for the same papers shown in Figure 11. The value of d was determined using the same process described above. For all the papers, the MD fluting had the lowest value of d=1.13 mm and the CD fluting had the largest value of d=8.8 mm. Figures 12 and 13 provide comparisons of the prediction from Equation (7) (vertical axis) and that using the equations of Mäkelä [17] (horizontal axis) for SENT specimens. The various markers represent different width webs, each with a/W= 0.005, 0.01, 0.015, and 0.025. The unrealistic web of W= 100 meters is given to demonstrate

Table 2. MD Properties of papers from [16 and 17] and prediction of d from Equation (6)

	Fluting	*Sack*	*News*	*Liner*	*MWC*	*SC*
TI kNm/kg	124	107	66	61.4	54.5	47
F, N	218	184	61.3	135	106	49.5
d mm	1.13	2.63	2.24	2.71	2.57	2.24
JI_{cr} Jm/kg	6.1	13.4	3.43	5.3	3.98	2.43

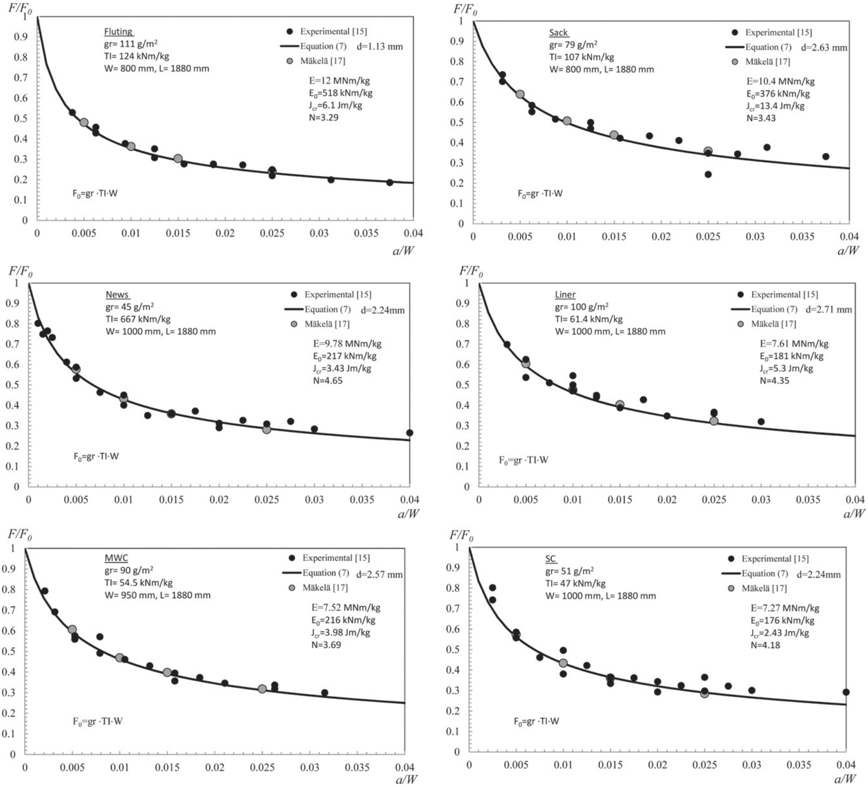

Figure 11. Comparison of LEFM results to experimental results from large webs [15], and the nonlinear fracture mechanics approach in [17].

that as the web width goes to infinity both solutions converge to that predicted from straight LEFM, which is shown as the dark dashed line. Once the web width gets small, the nonlinear fracture mechanics solution [17] diverges because the singularity at zero crack length remains in the solution. The current solution converges to the tensile strength for zero crack length.

Comparison of Figures 12 and 13 shows that the CD predictions is just as good as that for MD, even with a very large *FPZ* of d=8.8 mm. Figures 12 and 13 demonstrate that the modified LEFM theory is much better than classic LEFM, and because it converges to the tensile strength is likely a better fit than the nonlinear fracture mechanics solution for small sample widths or small crack lengths.

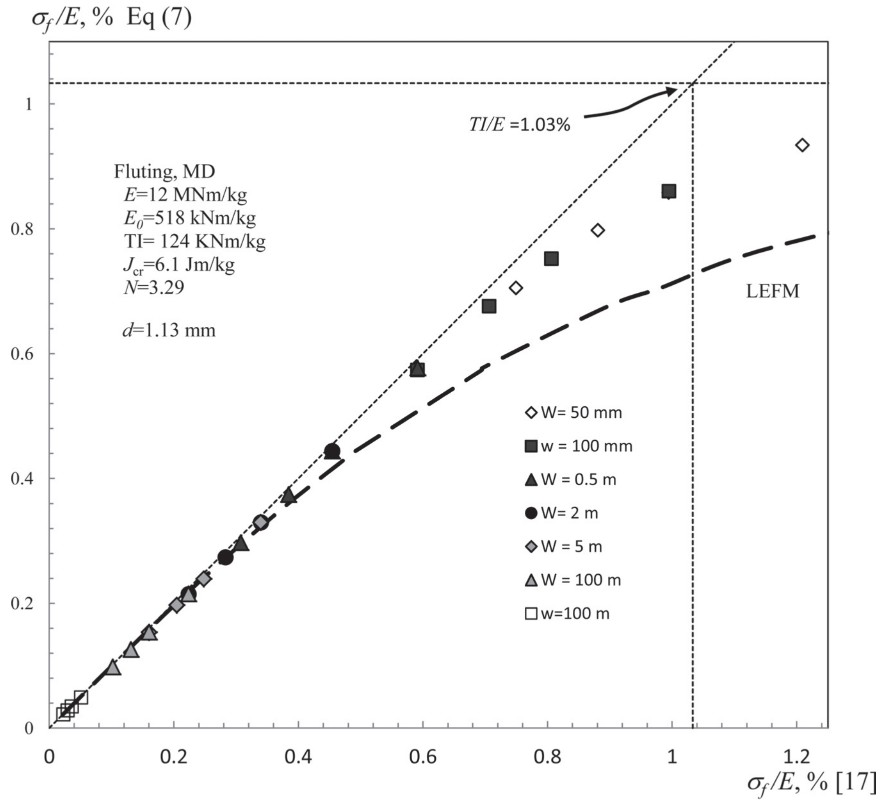

Figure 12. Comparison of Equation (6) with that from Reference [17] for MD Fluting.

The comparisons made in this section indicate that Equation (7) can be quite useful for characterization and prediction of the fracture sensitivity of papers. For the comparisons made here, only two parameters were needed, tensile strength, and the effective *FPZ, d*. The tensile strength is easily obtained from a standard tensile test, and *d* can be obtained from one fracture test. It appears that a 50 mm wide sample is sufficient for MD and CD at least up to a an *FPZ* of *d*=9 mm. Equation (7) has several advantages

- simplicity over methods of nonlinear fracture mechanics
- convergence to the tensile strength for small cracks
- predictive capabilities for a variety of commercial papers.

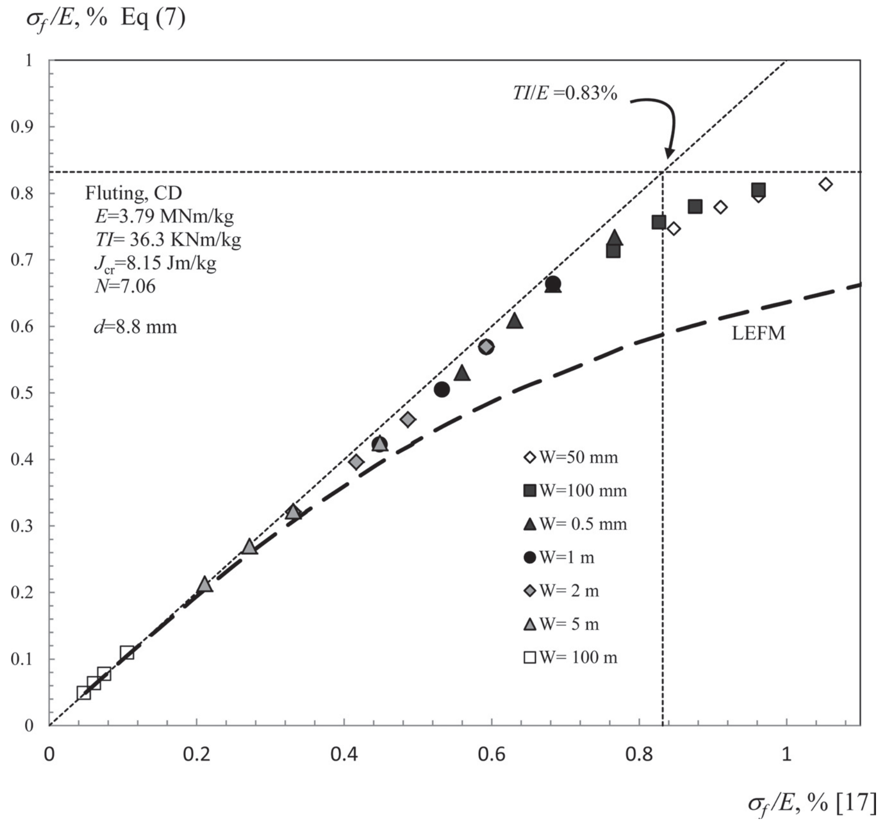

Figure 13. Comparison of Equation (6) with that from Reference [17] for CD Fluting.

4 EXPERIMENTAL

4.1 DENT Testing

A series of DENT fracture tests were conducted to further elucidate the modified LEFM model. The testing was completed on an Instron model 3344 universal tester, with pneumatic clamping. The grips were 76.2 mm wide and had serrated faces. The constant rate of displacement was 25.4 mm/min.

For samples that showed a tendency to break at the clamps, masking tape was used to reinforce the paper under the grips.

Sample dimensions varied but the typical test reported here used a width of 76.2 mm and a gage length of 180 mm. In reflection, MD sample lengths should probably be larger to ensure that the far field stress is more uniform, but conclusions remain the same. Samples were cut with both rotary and guillotine cutters with no significant differences found. Notches were cut prior to mounting with the use of either sharp scissors or a razor blade. Minimal differences in peak loads were found with different methods of sample preparation. For samples with small crack or ligament lengths, the size of the cut crack length was measured after the test.

All testing was conducted under constant environmental conditions of 50% Relative humidity and 22ºC.

4.2 Materials

A variety of commercial papers, a polymer film, and several handsheets were tested for fracture resistance. All samples were conditioned to 50% relative humidity and a temperature of 22ºC prior to testing. Properties of the commercial sheets are listed in Table 3. The papers represent a wide range of properties that one might expect from different grades. The grammage ranges from 22 to 200 g/m^2, the breaking length varies from 0.18 to 13.7 km, and the density varies from 170 to 1000 kg/m^3.

The stress-strain curves for the materials listed in Table 3 are given in Figures 14 and 15. The stress is normalized with the elastic modulus. The normalized stress was determined by dividing load by the maximum slope evaluated from the load versus strain curve. Strain was determined as change in length divided by original length.

Figure 14 shows that the MD and CD curves for both Newsprint and the Copy paper are essentially the same, except MD is more brittle than CD. The copy paper is more ductile than the newsprint and shows more yielding. The MD

Table 3. Physical Properties of Commercial sheets

	Grammage, g/m^2	*Density, kg/m^3*	*Tensile Index, MD*	*kNm/k CD*
Copy paper	77	770	51	34
Newsprint	46	630	58	12
Paperboard	200	640	75	28
Tissue Paper	22	170	1.8	1.4
Polypropylene	25	1000	134	—

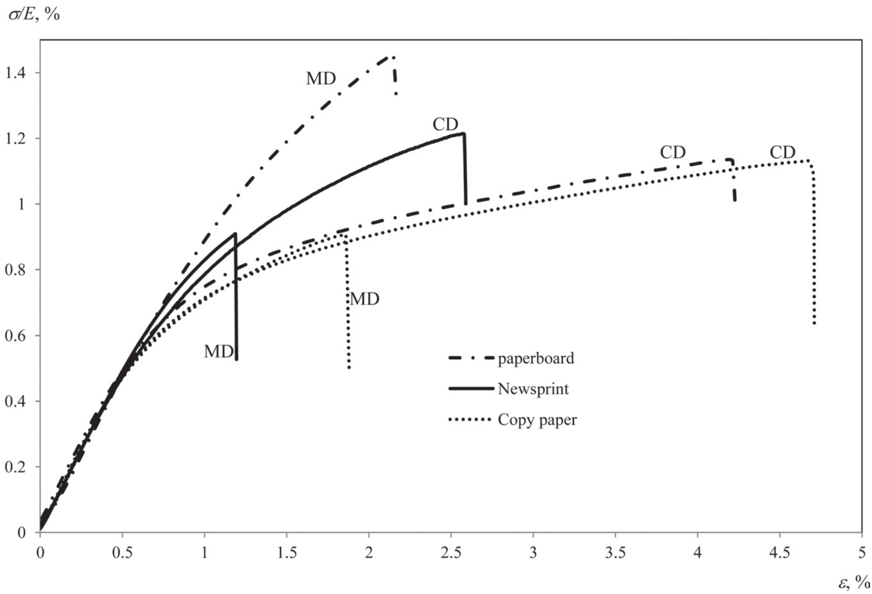

Figure 14. MD and CD Stress-strain curves for commercial papers. Stress is normalized to Elastic modulus.

paperboard has significantly less yielding and reaches a higher strength relative to its modulus than in the CD direction.

The tissue paper has high stretch (15%), and a very linear initial loading path for both MD and CD. This is because the tissue paper is in a bond-dominated regime with a very low breaking length and an equally low modulus. The polypropylene film has a well-defined yield point, followed by very slow strain hardening. The film is also quite ductile with a stretch of 150%. The CD paperboard curve is shown both in Figures 14 and 15 for reference.

Handsheets were produced on a 305 mm square Noble and Wood handsheet former. The pulp was NIST reference pulp 8495 (Northern Bleached Kraft Pulp). Beating was carried out in a Valley beater. Sheets were produced to three grammages, 25, 50, and 100 g/m^2. Pressing was carried out with a benchtop nip press and the sheets were dried on a drum dryer utilizing a tensioned fabric for restraint. Properties of the handsheets are given in Table 4. The focus of the handsheet investigation was to further investigate fracture resistance with large fracture process zones from structure; the emphasis was on no refining, low grammage, and low pressing.

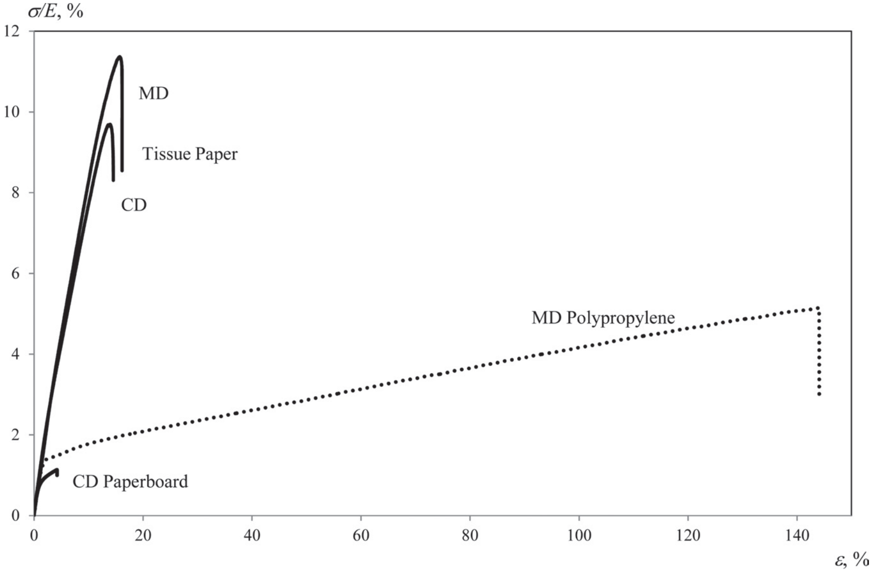

Figure 15. Stress-strain curves for tissue paper and polypropylene film. Stress is normalized to Elastic modulus.

Table 4. Properties of handsheets

CSF	*Grammage, g/m²*	*Density, kg/m³*	*Tensile Index, kNm/kg*	*pressing*
465	50	712	93	low
160	50	725	99	low
705	50	588	36	low
705	100	634	34	low
705	25	638	25	low
705	50	535	14	none

The stress-strain curves for the handsheets are given in Figure 16. Except of the CSF 160 and CSF 465 sheets, the sheets give a response where the efficiency of load transfer is so low that the scaled curves do not superimpose as well as one might expect [21].

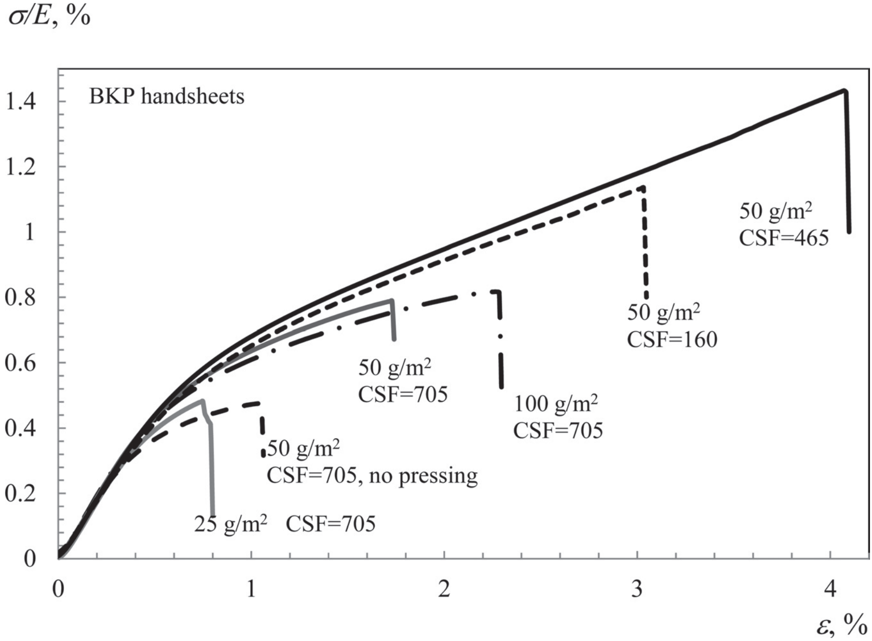

Figure 16. Stress-strain curves for handsheets.

5 RESULTS AND DISCUSSION

The focus of the DENT experiments was to determine if Equation (6) could be utilized to characterize the fracture behavior of a wide range of paper material responses, and if the structural contribution of the fracture process zone was necessary to explain the data. Figures 17–20 provide the results of DENT testing as well as fits using Equation (6). The parameters for the *FPZ* are given in Table 5. If the relative fracture resistance is due to inherent structure, one might expect $d=2d_s$, so the ratio is provided in Table 5.

Figures 17 and 18 show that Equation (6) well represents the fracture sensitivity for both MD and CD for a large range of crack sizes for both Newsprint and Copy paper. Equation (6) is a better fit for the Newsprint than the copy paper. For the copy paper, equation (6) under predicts the load ratio for deep notches or small ligament lengths as represented in the figures as small values of $1\text{-}a/w$. The newsprint appears to have a large contribution from the inherent structure rather than plasticity as observed by the large ratio of $2d_s/d$.

Table 5. Effective Fracture process zone, *d*, and structural zone length d_s for commercial sheets

		d, mm	d_s*, mm*	$(2d_s)/d$
Copy paper	MD	2.3	0.25	0.22
	CD	5.0	0.25	0.10
Newsprint	MD	1.8	0.8	0.89
	CD	4.0	2.0	1.00
Paperboard	MD	2.6	0.4	0.31
	CD	6.5	0.4	0.12
Tissue Paper	MD	4.2	1.7	0.81
	CD	7.0	2.5	0.71
Polypropylene	MD	0.23	0	0.00

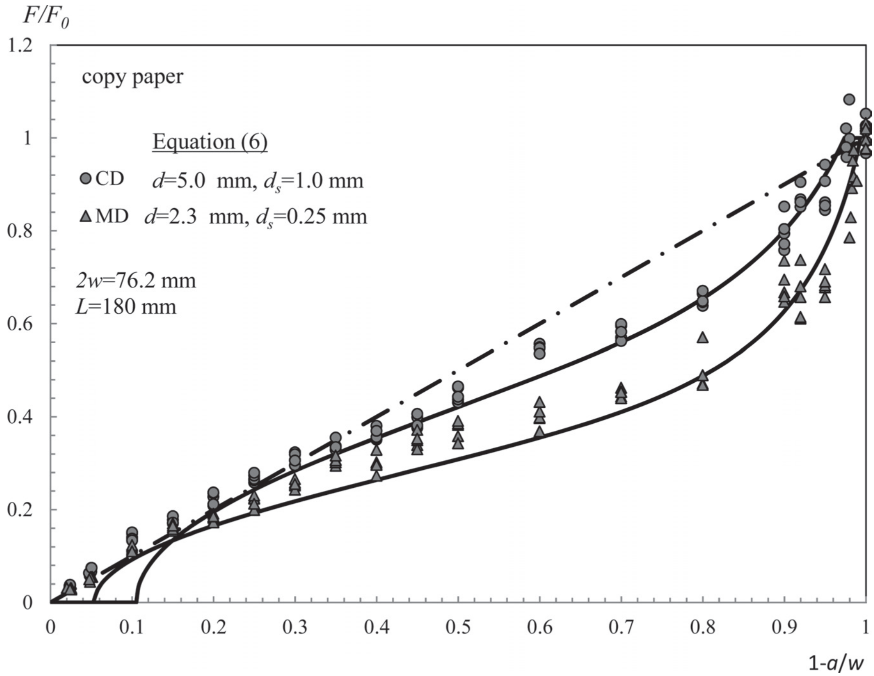

Figure 17. DENT results of load ratio versus relative ligament length for copy paper. Solid lines represent Equation (6). Dash-dot line represents notch-insensitive response F/F_0=1-*a*/*w*.

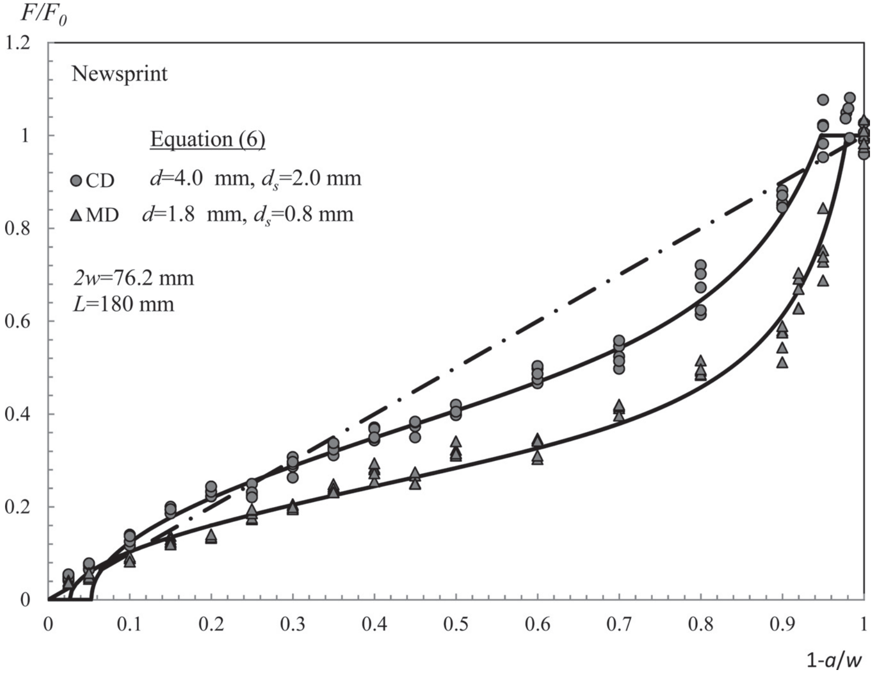

Figure 18. DENT results of load ratio versus relative ligament length for Newsprint. Solid lines represent Equation (6). Dash-dot line represents notch-insensitive response $F/F_0=1-a/w$.

Figure 19 shows that for MD DENT Equation (6) provides a reasonable representation of the behavior of the papers as well as the polypropylene film. For these materials, data was not collected for ligament length ratios less than 0.5. As one might expect, even though the polypropylene is by far the most ductile material tested, is has the most significant sensitivity to fracture. The value of d=0.23 mm suggests that the film can easily concentrate load and failure occurs at low far-field stresses. The tissue on the other hand has the least relative sensitivity to fracture and it is likely not due to plasticity of the fibers but the structure of the sheet as observed by the relatively high ratio of $2d_s/d$.

As shown in Figure 20 for CD (deep notches were not tested for CD), the fit of Equation (6) is reasonable, expect perhaps for the paperboard, for which the data forms a curve that cannot be fit well with Equation (6). Perhaps the cohesive failure mechanism for this paperboard in CD is much more dominate

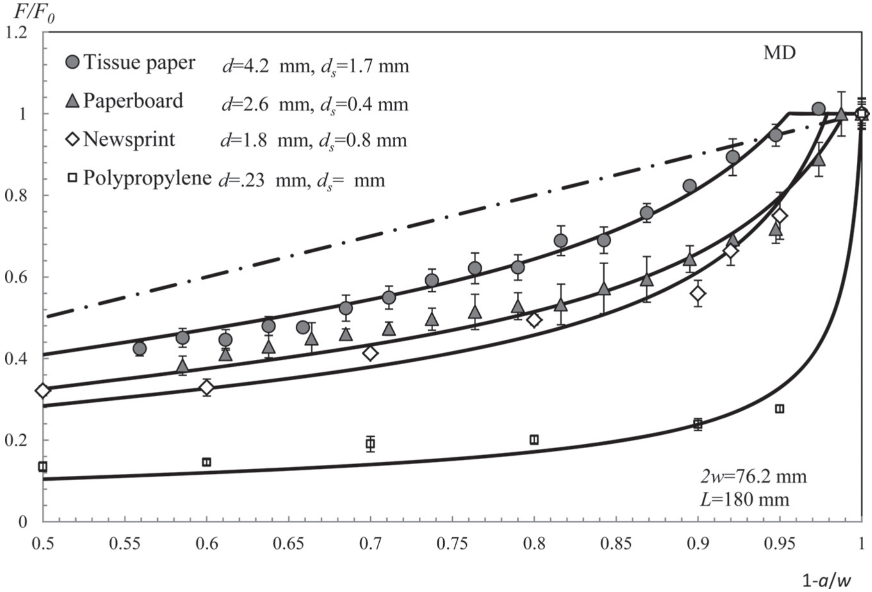

Figure 19. DENT results of load ratio versus relative ligament length for various papers in MD direction. Solid lines represent Equation (6). Dash-dot line represents notch-insensitive response F/F_0=1-a/w.

and the *FPZ* increases rather fast with crack size. Despite this poor fit, given the simplicity of the representation of Equation (6) it might be acceptable for practical considerations.

When one compares the MD and CD results, the clear trend is that MD is more sensitive to fracture than CD as indicted by the lower values of *d*. In addition, the inclusion of d_s is more important for CD compared to MD. For larger cracks sizes d_s can be ignored.

Bither and Waterhouse [22] showed that handsheets produced from unbeaten pulps showed little fracture sensitivity, but as the pulp was beaten, the sensitivity to fracture increased. Their sample width was rather small, 25.4 mm, so the fracture process zone could have been too large for the unbeaten pulps. Seth and Page [21] effectively demonstrated that beating and wet pressing increased the efficiency in load transfer in the sheet. Low bonding leads to inefficiency. Conversely, as the efficiency in which the sheet carries load increases, the ability of the sheet to concentrate load would also likely increase. Therefore, relative fracture sensitivity would also likely increase. So even though fracture toughness might increase with beating, the fracture process zone would likely decrease.

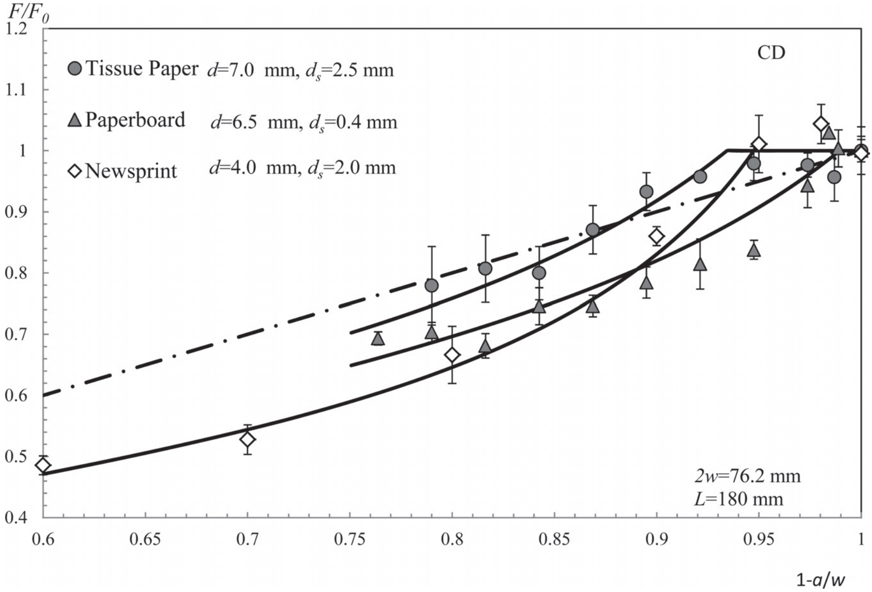

Figure 20. DENT results of load ratio versus relative ligament length for various papers in CD direction. Solid lines represent Equation (6). Dash-dot line represents notch-insensitive response F/F_0=1-a/w.

Therefore, for unbeaten sheets the fracture sensitivity relative to the tensile strength would be lower.

The DENT results for the handsheets, as shown in Figures 21 to 23 reinforce the concept that the loss of efficiency increases the area of paper activated in a fracture process, and thus, the relative sensitivity to fracture decreases. For well bonded sheets, the *FPZ* is smaller and the relative sensitivity increases. Figure 21 shows that the two sheet made from beaten pulp have small effective *FPZ* of about d=2 mm, while the unbeaten pulp has an effective *FPZ* of d=5 mm. If one considers the stress-strain curves previously given in Figure 16, the two beaten pulps have much better developed stress-strain curves, and represent good transfer of load to fibers. Following the same line of reasoning, Figure 22 demonstrates that un-pressed sheets further increases *FPZ* and the structural contribution d_s.

Figure 23 demonstrates that lower grammage sheets have increased relative fracture resistance. One would expect that with low grammage sheets, coverage is low, the bonded area is low, surface fibers make up a significant portion of the sheet, and thus, load transfer is impeded. This increases the *FPZ* and thus increases relative fracture resistance.

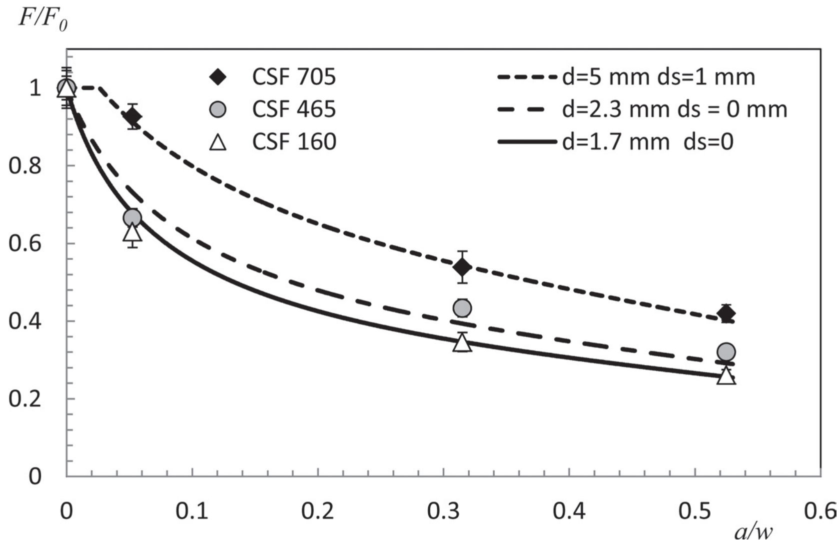

Figure 21. Effect of beating on DENT fracture sensitivity for handsheets, 50 g/m^2.

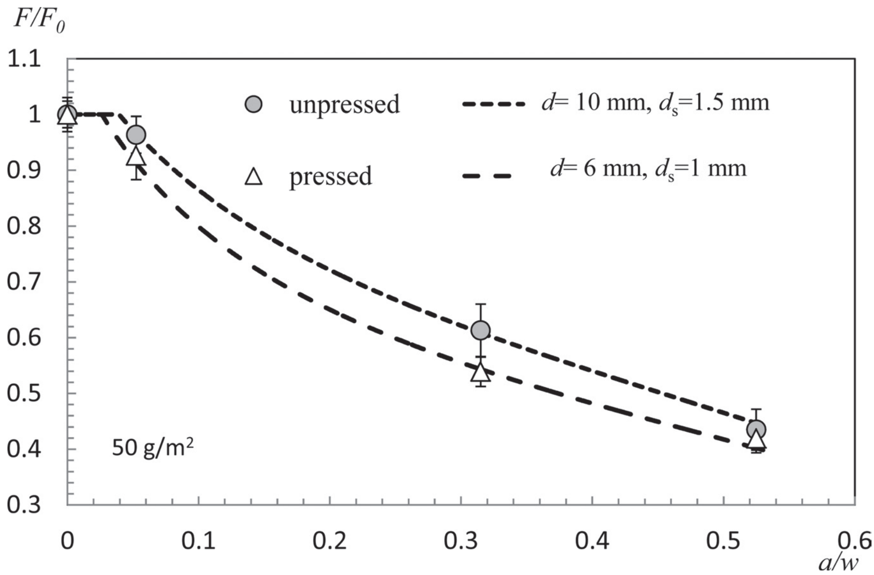

Figure 22. Effect of pressing on fracture sensitivity of handsheets made from unbeaten pulp.

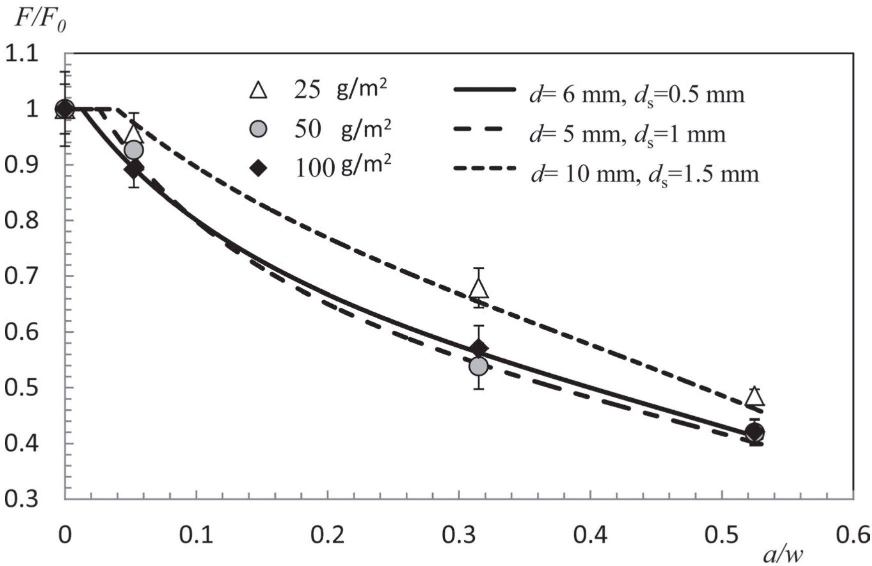

Figure 23. Influence of grammage on fracture sensitivity of handsheets from unbeaten pulp.

The results given above suggest that the effective fracture process zone, *d*, can be used as an indication of the relative fracture sensitivity of the sheet. As the load transfer efficiency is increased by means of improved bonding through beating and pressing, the stress-strain curve can be developed but relative fracture resistance decreases. The decrease in fracture process zone is indicative of an increase in the sheet's ability to concentrate load. The stress intensity factor would be affected by both the tensile strength and the magnitude of the fracture process zone.

Swinehart and Broek [8] showed that sample scaling with LEFM held at least for wide webs and large cracks. The results from [6] as shown in Figure 7 suggest that scaling holds for narrow widths too. The results given in Figure 11 demonstrated that calculating the effective process zone from a 50 mm wide sample was sufficient to predict fracture loads for small cracks in large webs. The ability of a narrow width samples to provide an estimate of the fracture process zone depends on the magnitude of the *FPZ*. If the zone is small, say *d*=1.0 mm, then even a sample width of 15 mm should be adequate for cracks up to *a*=4mm, a width of 25 mm should be valid for cracks up to *a*=10 mm. For a large fracture process zone, *d*=10mm, a sample width of 50 mm should be valid for cuts up to *a*=8 mm.

Figure 24 shows results for MD specimens of copy paper with widths of 25.4, 50.8, and 76.2 mm width along with the curves given by Equation (6). These results demonstrate that with d=2.3 mm, the scaling predicted from Equation (6) is reasonable, and this should hold for larger webs. Figure 25 shows the results for CD. With d=5 mm, Equation (6) does not hold as well for the 25.4 mm width, but it is adequate for the two larger widths. Even for the 25.4 mm wide web, Equation (6) is reasonable for cracks less than 6 mm. Figure 17 shows that this fit is adequate for the 76.2 mm wide web for cuts up to a=34 mm or a ligament length of about 8 mm. The actual CD fracture load is larger than that predicted by Equation (6) for these deep cracks. For larger webs, it is likely that the prediction from Equation (6) would be valid for deep cuts and would most likely be a conservative under-estimate of the fracture strength.

For DENT samples where the ligament length is in the range of d to $3d$, the average ligament stress likely exceeds the tensile strength of the material as demonstrated by the results of Tanaka and Yamauchi [23]. The plastic zone length

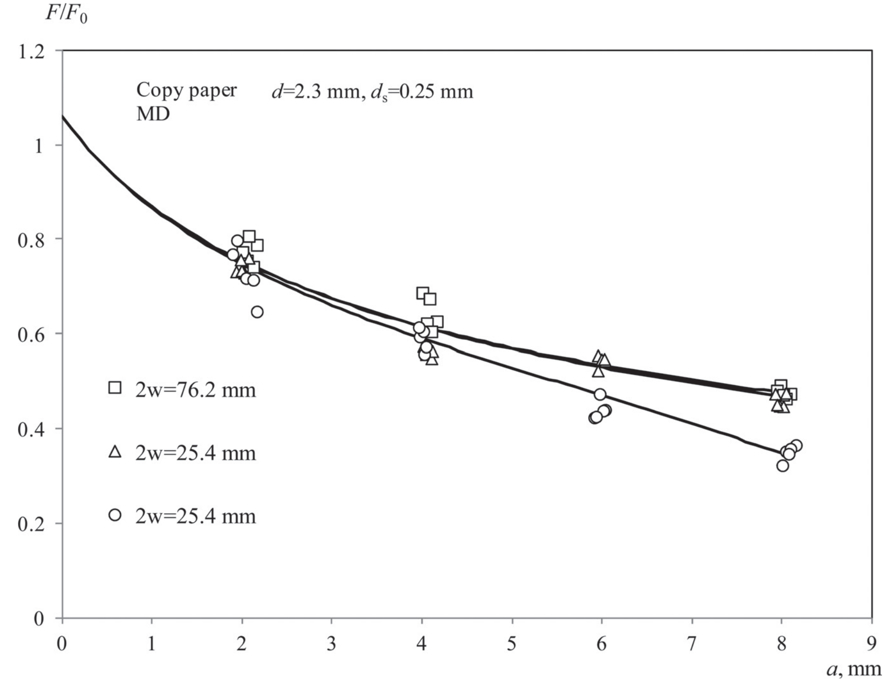

Figure 24. Fracture versus crack length for three widths. MD copy paper.

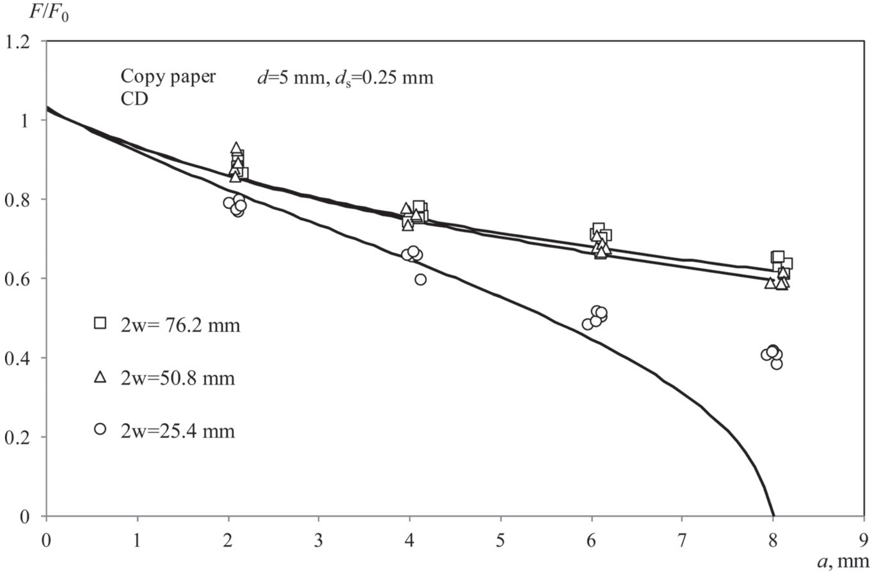

Figure 25. Fracture load versus crack length for three widths. Copy Paper CD.

determined by Tanaka and Yamauchi [23] from DENT tests with the ligament length one third the sample width can be recalculated to give the ratio of average ligament stress to tensile strength. They varied the width from 3 to 63 mm and their results show that the average ligament strength can exceed the tensile strength by an additional sixty percent. For example, for newsprint a ligament length of 2 mm gave a ligament stress that was 1.3 the tensile strength in MD and 1.5 the tensile strength in CD. This indicates that the intrinsic strength of the sample is higher than the measured tensile strength and that tensile strength is limited by fracture due to the cutting of the structure at the edges. With a DENT sample, fibers crossing the ligament form a path for load transfer. The same fiber cut at the edge of a sample would lose much of its ability to carry load. For smaller ligament lengths, the fracture process zones superimpose, stress concentrations are lower and the measure of fracture load is a better estimate of intrinsic tensile strength of the network.

Figure 26 provides the ratio of fracture ligament stress to tensile strength for four sample types of MD copy paper. Three of the samples are tensile strips (a=0) with three widths, 25.4, 75.2, and 2.5 mm. The fourth sample is a DENT with a ligament length of 2.5 mm. The DENT sample has a strength that is 47% larger than the tensile strength of the sample. This suggests that without a notch, the

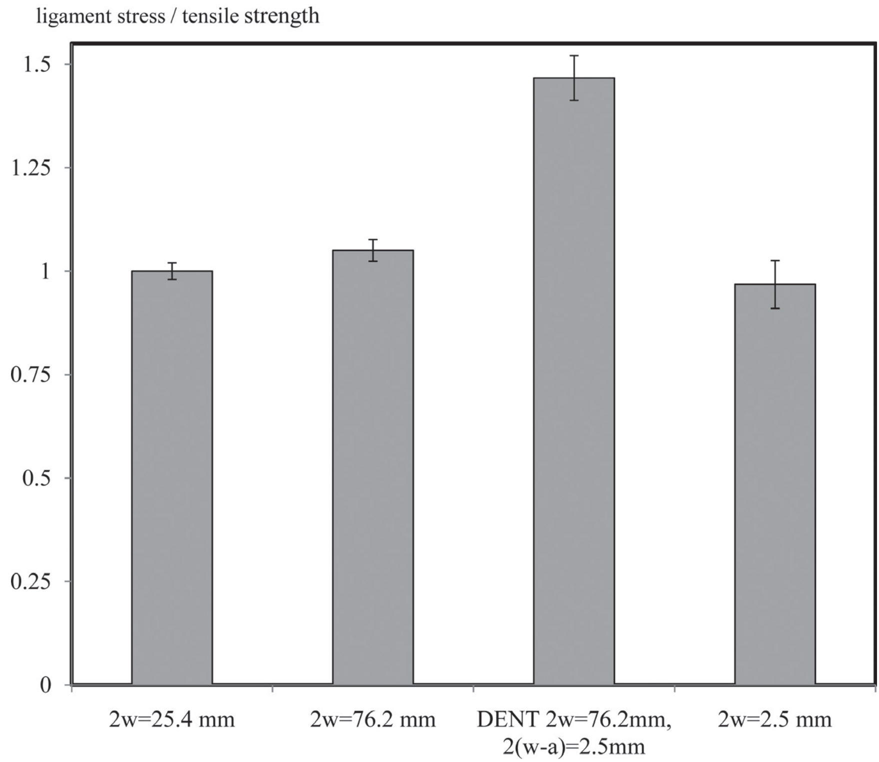

Figure 26. Comparison of tensile strength versus deep-notched DENT strength for MD copy paper.

sample fractures at the edges because of inherent flaws in the structure, which are opened up when the edges are cut. The structure in the ligament of the DENT sample is intact and can carry significantly more load.

6 CONCLUSIONS

Contrary to statements in the literature, it was found that a modified linear elastic fracture mechanics (LEFM) model can be applied to paper for both materials characterization and prediction. By using a ratio of fracture loads from LEFM equations, fracture resistance can be determined from the tensile strength and an effective fracture process zone, d. The fracture process zone can further be split to a structural, d_s, and a materials component, although this separation is not needed for the majority of cases to obtain reasonable predictions. Equation (6) proved useful in characterizing a wide range of papers from tissue to paperboard for both MD and CD. For most papers, a 50 mm sample width should be sufficient to characterize the materials fracture sensitivity. Results from small samples should scale to large webs at least until the crack depth is quite deep. Simplicity of application is the great advantage offered by the modified LEFM compared to other available methods.

The current results support the previous work of Donner [8] linking the tensile strength directly to the fracture behavior and suggesting that the inherent network structure of paper contributes to fracture toughness. As sheet efficiency decreases, tensile strength decreases, but the effective fracture process zones increases, thus the relative fracture toughness increases. In many cases the actual fracture toughness would decrease because the loss of strength exceeds the gains from an increased fracture process zone.

For a wide range of commercial papers, the effective fracture process zone was in the range of 1 to 3 mm for MD and only larger, about 4 mm, for tissue papers. In CD, the fracture process zone was found to be in the range of 4 to 9 mm for all papers investigated. For tissue papers, which tend to be low grammage and bond-strength dominated, the fracture toughness appears to be structural, a result of a large fracture process zone resulting from poor transfer of load. For newsprint, structure also appears to dominate the fracture toughness as indicated by the ratio of $2d_s/d$ near unity. For other papers, plasticity of the fibers probably plays a larger role in fracture toughness.

Although material plasticity plays an important role in fracture toughness, the material with the largest sensitivity to fracture was the polymer film with a stretch of 150%. That is because the ability of the sheet to concentrate load plays an even greater role in determining fracture toughness. The polymer film can concentrate load much better than paper's fiber network, and thus when a crack is introduced in the film, the stresses near the tip reach failure loads when the far field load is still quite low. In paper, the network structure impedes the ability of the sheet to concentrate stress and as a result the relative resistance to fracture is much higher. The effective fracture process zone can be considered as an indicator of how well the sheet can concentrate load. The smaller the value of d, the better the sheet can concentrate load. Even if the material were perfectly elastic and brittle, increasing the characteristic length of the structure would improve the relative fracture resistance.

The edges of a paper are inherently flawed because the structure is disrupted by cutting fibers that cross the edge. The tensile strength is then a result of fracture resulting from concentrated loads as some point where the edge flaw is largest (This assumes that no larger defects like a large shive or a hole are in the interior of the sheet). The notches or cracks introduced in a DENT cause the average stress over the ligament to be high and failure initiates at one or both of the notch tips. The process of cutting a slit induces little damage to the network structure remaining in the ligament. Thus the inherent strength of the sheet can be determined from deeply notch specimens and can easily be 50% greater than the tensile strength.

The second advantage to using the modified LEFM equation presented here, Equation (7), is that the singularity at small crack lengths is eliminated. The reason that LEFM was dismissed is that it over predicts the fracture strength for small cracks as evidenced by the literature where LEFM does a better job of predicting CD compared to MD even though CD has more plasticity associated with it. The modification presented here ratios the load to the tensile strength, which is determined from the effective fracture zone and thus insures reasonable convergence for small crack lengths. This actually provides a better estimate then other models that include plasticity but leave the singularity at zero-crack length. It is important to note that the current LEFM modification does not make use of the yield stress but rather assumes the tensile strength is also a result of fracture. The comparison to experimental results supports this assumption.

Finally, we conclude that by embracing the use of LEFM to describe the fracture resistance of paper, one can obtain new insights into the role of materials and structure to the observed mechanical behavior of paper.

ACKNOWLEDGEMENT

The authors thank Petri Mäkelä for kindly providing the experimental data from [15], which was utilized in Figure 11 and his personal communication on limitations of existing models due to stress singularities.

REFERENCES

1. M. T. Kortschot. "Fracture of Paper", in *Handbook of Physical Testing of Paper*, editors R. E Mark, C. C. Habeger, J. Borch, and M. B. Lyne, Marcel Dekker, vol. 1, edition 2, 429–480, (2001).
2. P. Mäkelä, "On the fracture mechanics of paper," *Nordic Pulp and Pap Res J.* **17**(3):254–274 (2002).
3. K. Niskanen. "Strength and fracture of paper," *Products of Papermaking, Trans. Xth Fund. Res. Symp. Oxford*, 1993, (C.F. Baker, ed.), pp 641–725 (1993)
4. S. Östlund and P. Mäkelä, "Fracture Properties," *Mechanics of Paper Products*, Ed. K. Niskanen, De Gruyter, Germany, 67–89 (2012)
5. T. Uesaka, H Okaniwa, K. Murakami, and R. Imamura, "Tearing Resistance of Paper and its Characterization, *Japan Tappi* **33**:403–409 (1979)

6. S. Östlund, K. Niskanen, P. Kärenlampi, “On the Prediction of the Strength of Paper Structures with a Flaw,” *J of Pulp and Pap Sci*, **25**(10):J356–J360 (1999)
7. R. S. Seth and D. H. Page, “Fracture Resistance of Paper, *J Mats Sci* **9**:1745–1753 (1974).
8. D. Swinehart and D. Broek, “Tenacity and Fracture Toughness of Paper and Board,” *J of Pulp and Pap Sci*, **21**(11):J389–J397 (1995)
9. B.C. Donner. “An heuristic model of paper rupture,” *The Fundamentals of Papermaking Materials, Trans. XIth Fund. Res. Symp. Cambridge, 1997*, (C.F. Baker, ed.), pp 1215–1247 (1997) (C.F. Baker, ed.), pp 1215–1247, FRC, Manchester, 2003.
10. O. Andersson and O. Falk, “Spontaneous Crack Formation in Paper,” *Svensk Papperstidning* **69**(4):91–99 (1966)
11. K. Niskanen H. Kettunen, and Y. Yu, “Damage Width: a measure of the size of the fracture process zone,” *Proceedings of the Science of Papermaking, 12th Fundamental Research Symposium*, Oxford UK, pp. 1467–1482 (2001).
12. D. Hristopulos and T. Uesaka, “Structural disorder effects on the tensile strength distribution of heterogenous brittle materials with emphasis on fiber networks,” *Physical Review B* **70**: 1–18 (2004).
13. M. T. Kortschot and K. Trakas, “Predicting the strength of paper containing holes or cracks with the point stress criterion,” *TAPPI J* **81**(1): 254–259 (1998)
14. J. M. Considine, D. W. Vahey, J. W. Evans, K. T. Turner, and R. E. Rowlands, “Evaluation of strength-controlling defects in paper by stress concentration analyses,” *Journal of Composite Materials*, **46**(11):1323–1334 (2011)
15. P. Mäkelä, H. Nordhagen, and O. W. Gregerson, “Validation of isotropic deformation theory for fracture mechanics analysis of paper materials,” *Nordic Pulp and Paper Research Journal*, **24**:388–394 (2009).
16. P Mäkelä, and C. Fellers, “An analytic procedure for determination of fracture toughness of paper materials,” *Nordic Pulp Paper Res. J.* **27**(2), 352–360 (2012)
17. P. Mäkelä, “Engineering fracture mechanics analysis of paper materials,” *Nordic Pulp and Paper Research Journal* **27**(2):361–369 (2012)
18. P. Isaksson, P.J.J. Dumont, S. Rolland du Roscoat, “Crack growth in planar elastic fiber materials,” *International Journal of Solids and Structures* **49**:1900–1907 (2012).
19. H. Tada, P. C. Paris, and G. R. Irwin, *The Stress Analysis of Cracks Handbook*,” 3rd edition, ASME Press (2000)
20. D. E. Swinehart and D. Broek, “Tenacity©, fracture mechanics, and unknown coater web breaks, *Tappi Journal* **79**(2):233–237 (1995).
21. Seth, R. S. and Page, D.H. (1981): “The stress-strain curve of paper”, *The Role of Fundamental Research in Paper Making, Trans. of the .7th Fund. Res. Symp.*, Cambridge, 1981, (J. Brander, ed.), pp 421–452, FRC.
22. T. W. Bither and J. F. Waterhouse, “Strength development thought refining and wet pressing,” *TAPPI Journal* **75**(11):201–208 (1992).
23. A. Tanaka and T Yamauchi, “Size Estimation of Plastic Deformation Zone at the Crack Tip of Paper Under Fracture Toughness Testing,” *J Pack Sci Tech* **6**(5):268–277 (1997).

Transcription of Discussion

UTILIZATION OF MODIFIED LINEAR ELASTIC FRACTURE MECHANICS TO CHARACTERIZE THE FRACTURE RESISTANCE OF PAPER

Douglas W. Coffin[1], *Kun Li*[2] *and Ji Li*[1]

[1] Department of Chemical and Paper Engineering, Miami University, Oxford OH 45056 USA
[2] Metso USA, Norcross, GA 30071 USA

Petri Mäkelä Tetra Pak

Thank you for a nice presentation and an interesting paper. Could you please re-show one of the first equations in your presentation, the one that is called Equation 4 in your article. This expression can be used to evaluate the tensile strength for a given tensile test piece size, when the parameters K_I and d are known. As I understand it, you assume that the parameters K_I and d are constants. Wouldn't this imply that the expression predicts that the tensile strength is dependent on the test piece width?

Doug Coffin

It will change slightly because of the scaling. Using Equation (4) with the shape function for the double-edge notched tests, the difference in tensile strength is quite small as width is increased.

Petri Mäkelä

The equation predicts that the tensile strength increases when the test piece width is increased. That feels a bit odd, since experiments generally show that the tensile strength is independent of the test piece width or even that the tensile strength is reduced for wide test pieces, as predicted by weakest link theory.

Doug Coffin

No, because, with small enough values of inherent crack length, *d*, *d*/*w* approaches zero giving a constant shape correction factor at all but the smallest widths and, as the width increases, the value of *d*/*w* goes to zero and the shape correction factor converges to a constant value.

Petri Mäkelä

But if you have *d* as a constant and you gradually increase the width of the test piece, this expression says that the tensile strength increases with test piece width.

Doug Coffin

No because the *d* gets so small compared to *w*, *d*/*w* it goes to 0, and *f(d/w)* converges.

Petri Mäkelä

I'll put in the numbers and check it. Have you considered assuming that the tensile strength is a constant, while the parameter *d* is used as a free parameter? There is also experimental evidence that the cohesive zone increases when you increase the width.

Doug Coffin

That is true. When you have large cracks, I agree with you, that is going to change and it is going to slightly change that curve. But how important is it? Yes and clearly as the notch depth is increased, the actual fracture strength is probably going to level out. I agree with that, but your model is not capturing that either. It would take a change in the cohesive zone for deep notches.

Petri Mäkelä

I have one additional comment, Doug, concerning the equation on the next page in your presentation, the one that is denoted Equation 5 in your article. This expression allows for evaluation of the limit load ratio by relating the limit loads for one un-notched and one notched test piece that are subjected to tension. You state in the article that this equation converges to unity when the notch size, denoted by the parameter *a*, equals zero. However, in a typical real practical situation, the un-notched tensile test is performed for a small test piece in the lab, while the target is to predict the limit load for a large notched paper web. This means that the un-notched and notched configurations have different widths. Such transferability can only be handled by Equation 5 if the two instances of the width in the expression, denoted by *w*, are allowed to have different values. Under such conditions, Equation 5 will no longer predict unity for zero notch size.

Doug Coffin

That is true, but again it is a matter of significance. The results shown here illustrate that it is not that important. Say $d = 4$ mm, the difference in tensile strength between a sample at 25 mm and 1000 mm is less than 5%. The variability in data at the same width is of that order, so I think to first order it is not that important.

Warren Batchelor Monash University (from the chair)

I was not quite clear how you determined all the different values of *d*, maybe there is something I missed.

Doug Coffin

No, that is fine. So, we have a measurement for tensile strength, and we have data that is collected. So there is only one parameter, so you calculate *d* to get the best fit of the data. To get the curves (variable width data), the *d* was taken from the previous data and these tests were conducted at the different widths; then, using that same *d*, you get a good prediction (showing that scaling works). For the data from the literature, the *d* is determined from the data for the one fracture test that Petri Mäkelä did. Then you get the curve that fits the other wider width test. So you need a tensile strength and one other fracture test at least, and it has to be one appropriate fracture test and it has to be of a size where there is no overlapping of the fracture process zones.

Mikael Magnusson KTH

This *d* parameter, if I understand it correctly, you see it as a fitting parameter; but it can also be physically interpreted. I think you mentioned that it is more or less the diameter of the process zone. Since you tested quite a few different materials, would it be possible to link *d* to, perhaps, fibre length or the length of a couple of fibre segments in a test?

Discussion

Doug *Coffin*

I do not look at d as a fitting parameter, it is a characteristic of the sheet or a material property obtained from a fracture test.

What you suggest is possible. I would say that d_s is the structural part, but it is not just a fibre length but the fibre length and how well it is bonded into the sheet The d is how much of the paper is activated to progress the crack, so it has to do with how well things are bonded, or importantly bonded systems. Perhaps fibre length, and perhaps floc length is in there, because, in order to deform it, you've got to activate a large part of the region to get the crack to drive through. So that is why for the papers which are not well bonded, the fracture points are so large and it takes a lot of area: a lot of areas being pulled out to progress the crack. In those with high strengths, where there is a lot of bonding, the fracture process zone is lower because you can concentrate the stress. So to tie it to fibre length, there could be some correlation but there does not have to be. So I looked at d_s as a function of density and clearly as the density goes up, the d_s parameter goes down and you could possibly draw a line if you wanted. So if you densify the structure you get better bonding and you can concentrate load better, you can concentrate energy better and it is going to be more sensitive to fracture. But, I would hate to say that it is actually just the fibre length.